Colloid Polym Sci 278:406–417 (2000)

ORIGINAL CONTRIBUTION

P. Chodanowski
S. Stoll

Collapse transitions of a supersized neutral chain due to irreversibly adsorbed small colloidal particles

Received: 26 July 1999
Accepted in revised form: 9 November 1999

P. Chodanowski · S. Stoll (✉)
Analytical and Biophysical
Environmental Chemistry (CABE)
Department of Inorganic
Analytical and Applied Chemistry
University of Geneva, Sciences II
30 quai E. Ansermet, CH – 1211
Geneva 4, Switzerland
e-mail: serge.stoll@cabe.unige.ch

Abstract We performed Monte Carlo simulations to study the destabilization processes of large neutral and flexible polymer chains due to irreversibly adsorbed colloidal particles attached to the chains like beads on a necklace. The particles are modeled as charged spherical units which interact with each other via repulsive electrostatic and attractive van der Waals (vdW) potentials. The usual Monte Carlo search procedure is extended and carefully checked to completely sample the chain conformational space and achieve dense conformations in the limit of both strong attractive and repulsive interaction potentials. Configurational properties, such as the radius of gyration, the end-to-end length, and the Kuhn length, are calculated as a function of the intensity of the vdW interactions and ionic strength values. It is observed that chains exhibit a new range of possible conformations compared to the classical random walk and self avoiding walk chains or polyelectrolytes. In the limit of low salt concentration, by gradually increasing vdW interactions, chains undergo a cascade of transitions from extended structures to dumbbells, from dumbbells to pearl necklaces, and from pearl necklaces to collapsed coils. Because of strong competition between the vdW and electrostatic forces, the distance along the chain between the interacting particles, and the sampling limitations, these transitions are found to sample metastable domains and to depend on the initial conformations. To gain insight into the spatial organization of the collapsed conformations, the pair correlation functions of both monomers and particles are calculated. It is shown that collapsed conformations which are the result of strong particle–particle interactions exhibit two distinct parts: a hard core mainly composed of particles and a surrounding polymeric shell composed of loops and tails. Possible effects of such a collapsed transition on the kinetics of flocculation of a mixture containing large flexible chains and small adsorbing colloidal particles are discussed.

Key words Polymer conformation · Adsorbed colloidal particles · Monte Carlo simulations · Collapse transition

Introduction

The flocculation of colloidal particles by polymers [1] is a process of a great practical and theoretical importance in colloid science, as well as in the chemical and physical regulation of major compounds such as pesticides and trace metals in aquatic systems [2–4]. In natural waters containing mixtures of inorganic colloids and polymers originating from many sources (algae, microorganisms, phytoplankton cells), floc formation occurs between sub-micrometer-sized mineral particles (clays, silicates, iron and manganese oxides) and supersized extracellular polymers (Fig. 1) such as polysaccharides, which represent 80–90% of the total extracellular material [5, 6]. When the floc size or the mass is large enough, the flocs are eliminated from the water column by a sedimentation process [7, 8]. Thus, flocculation acts as one of the key physicochemical regulation processes of the concentration, transport, and fate of colloidal matter and of associated vital or toxic trace metals and compounds in natural waters.

Nonetheless, the process of flocculation is very complex since it often consists of many steps in the formation of large flocs (aggregate formation while passing by the formation of elementary structures, restructuration, breakup, etc.) which are difficult to distinguish in experiments [9, 10]. It should be noted that, prior to the emergence of large flocs, the formation

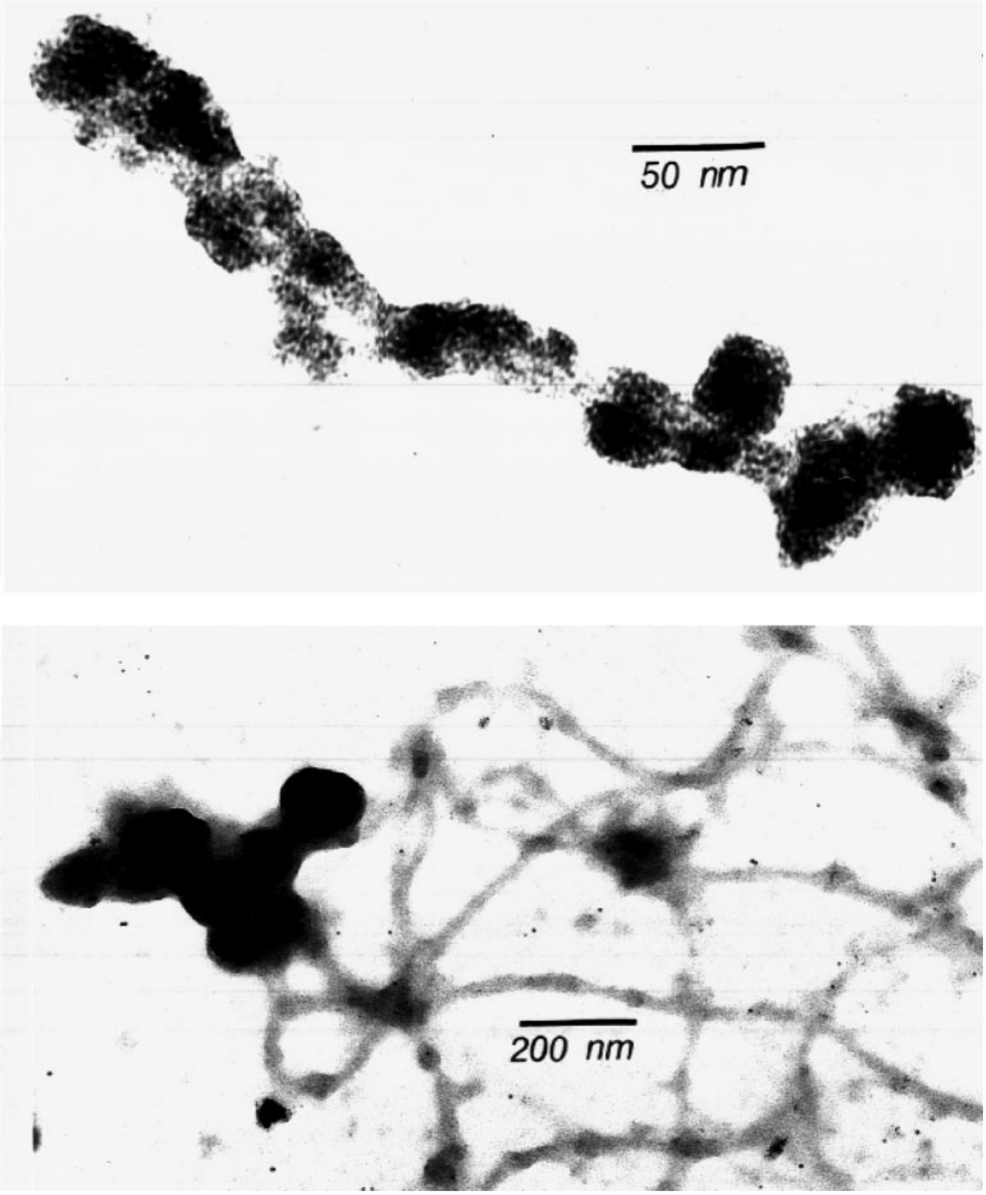

Fig. 1 Transmission electron microscope image highlighting the possible associations between small inorganic colloids and large organic macromolecules in natural waters. Magnification of natural water samples from a small eutropic lake (Lac de Bret, Switzerland) prepared by ultracentrifugation into a hydrophobic resin and Ag/Mo/Cu poststaining. The poststaining technique has been developed to avoid potential conformational changes due to the direct addition of stains to the samples. In effect, low stain concentrations are employed only once the colloids are embedded in a hydrophilic resin

of elementary structures is expected. It has been shown with the help of mathematical modeling [11] that aggregates (referred to as type I) composed of colloidal particles only, as well as aggregates consisting of a single chain associated with one or more particles (type II), are rapidly formed (first regime of floc formation) owing to the high specific surface area of the chains and the high diffusion coefficient of the free particles. In a second regime of floc formation, types I and II collide with each other or with naked chains to form, via particle bridges, larger structures composed of several chains, denoted type III aggregates. The stability and structures of type I aggregates in terms of reaction-limited aggregation and diffusion-limited aggregation concepts, as well as the possible aggregate fragmentation and restructuring, have been intensively discussed in the literature [12–16] and have proven to be reasonably well described by the von Smoluchowski kinetics based on mean field approximations [17] and computer modeling [18, 19]. However, there has been little discussion of the stability and the possible conformational changes of supersized chains on which particles are adsorbed (type II aggregates) in the first flocculation regime. In particular, if particle adsorption induces chain reconformation, large changes in the chain dimensions are expected to profoundly affect the kinetics of flocculation as well as the floc structures (density, porosity, internal cohesion) and floc settling properties.

It is generally accepted that the basic mechanism of flocculation of colloidal particles by polymers is a bridging process in which the polymer acts by adsorption on the surfaces of two or more particles forming bridges between particles. Several theoretical models based on scaling concepts were developed to describe such adsorption processes. Using a scaling description of the confinement energy of the chain steric stabilization mechanisms to mimic the presence of a supersized chain interacting with small particles, the adsorption energy and the dimensions of a single chain adsorbed on a sphere as a function of the sphere radius, chain length, and strength of the adsorption were proposed [20, 21]. The idea was to apply the same concepts to adsorption on small objects whose surface area is too small to allow the polymer to spread to the extent corresponding to the same parameters on a free surface. Such models were used, in particular, to explain the adsorption of hydrophobic polymers on micelles [22–24]; however, the higher the molecular weight of the polymer, the more difficult the problem becomes in terms of the cited theories to reconcile them with experimental observations. As demonstrated by Cabane and coworkers [25–27] and by Currie and van der Gucht [28] by considering the effect of adsorbed macromolecules on the interactions between surfactant micelles, microemulsion droplets, or solid spheres dispersed in a liquid, when the size of a polymer chain is comparable to or greater than the size of colloidal particles, one has to reevaluate the flocculation process by considering the attachment of particles to polymers rather than adsorption of polymers onto particles.

Computer simulations of colloid and chain interactions are expected to provide a useful tool for investigating directly chain conformations before and after adsorption of small colloidal particles. Unfortunately, they are usually restricted to the classical picture of polymers of a rather small polymer segment number with regard to the size of the colloidal particles [29, 30]. As a result there are few reports on models involving supersized chains and comparatively small particles.

Nonetheless, a model was recently proposed to describe adsorption of fine particles by high-molecular-weight polymers and its effects on flocculation/sedimentation processes [31–33]. It was based on the assumption that the number of colloidal particles attached to a single polymer molecule is a random quantity and that a certain minimum number of particles must be attached to a macromolecule to cause its removal from the system. Although this model nicely elucidates the important deterioration of the ability of ultralarge polymers to flocculate fine suspensions, due to their rapid sedimentation when particles are attached to them, the static character of the model did not take into account the possible chain reconformation processes and the possible consequences which are expected to occur upon particle adsorption.

In a previous paper, we reported computer simulation studies [34] of two- and three-dimensional models for bridging flocculation between small colloidal particles and large linear polymer chains. The floc structures and formation kinetics as a function of the chain/particle concentration ratio, the chain conformation, and the space dimension were investigated to understand the key factors influencing flocculation in natural waters or wastewater treatment processes. The solution chemistry was chosen to emphasize particle–chain interactions compared to particle–particle or chain–chain interactions. Using rods and coils, it was shown how aggregation kinetics and floc structures are strongly dependent on and sensitive to the particle/chain concentration ratio and configurational properties of individual chains; however, chain conformations were assumed to be unchanged upon particle adsorption. As such effects were expected to greatly complicate the model and to increase the computational effort, monomer movements were not integrated in the equations of motion of the chains. Aware that reorganization processes arising from rotational motions of sequences of chains may be important in the intrinsic stability of flocs, provided chain reorganization processes are fast compared to the kinetics of aggregation and the macromolecule is "flexible" enough to allow conformational changes, the conformational changes of single chains in the presence of an arbitrary number of adsorbed colloidal particles are now reported here.

The present study uses a Monte Carlo (MC) model having the essential physical features capable of interpreting the effects of colloid adsorption on the conformation of polymer chains. The simulation method permits one to take into account the solution chemistry (ionic strength, temperature, pH) through van der Waals (vdW) and Coulombic interactions, which are of key importance in understanding chain structures as well as conformational transitions. The motion of sequences of chains is achieved with the use of a set of well-defined and classical monomer movements to sample the configurational space and to minimize the total energy of the chain–particle complex.

Unfortunately when large potentials are considered, i.e. when the ionic strength is close to zero or when vdW interactions between particles are important, most of the MC sampling procedures are poorly efficient for sampling the overall chain conformational space and extracting the most stable structures. This problem is of particular importance when chains have to achieve compact conformations because dense structures are rapidly entrapped in ‘‘frozen’’ conformations that have lower energy than nearby conformations but that have higher energy than more distant stable conformations since a few particle–particle contacts are required to greatly reduce the total energy of the chain into a local minimum. In order to improve the convergence rate, to achieve equilibrium conformations in a global minima, and to perform efficient sampling to obtain specific conformations, our sampling methodology was based on a MC configurational search sampling procedure which was successfully used to sample all the possible and exotic conformations of strong hydrophobic polyelectrolytes [35].

Model

To model a linear, neutral, and flexible chain on which several small charged colloidal particles are irreversibily adsorbed, chains are represented as an off-lattice three-dimensional necklace consisting of hard spheres standing for physical monomers, along which spherical units are included to mimic the presence of adsorbed colloidal particles (Fig. 2). Each physical monomer is considered to be neutral and to have a bond length of 7.14 Å, whereas the particle diameter is set to twice the monomer diameter i.e. 14.28 Å. The model is not restricted to this set of values and permits the adjustment of the relative particle/monomer dimensions. The total number of units, i.e. particles and monomers, is 100 whereas 13 particles are arbitrarily fixed along the chain. The number of uncharged monomers between particles is between 6 and 9 along the chain to include a certain randomness in the particle location and to roughly minimize the electrostatic interactions.

Fig. 2 Schematic picture describing the neutral polymer chain on which several small charged colloidal particles have been attached. The particles are shown as large units connected to each other by monomers. Excluded volume, van der Waals and electrostatic interactions are included in the model to take into account the effects of particle–particle interactions versus solution chemistry. Surface charges of the particles are treated in the calculations as point charges

The inner part of the colloidal particles is assumed to have the same dielectric constant as the surrounding medium and no image effect is included in the model. The central point charge on the particle is fixed at +4 (0.2 C m^{-2}), which is a reasonable value for natural particles such as hematite at neutral pH [36]. The particle charge is kept constant with salt concentration. The solvent is modeled using a continuum approach with a dielectric permittivity constant, ε_r, of 78.5, modeling water.

Two particle–particle interaction potentials are considered: a long-range repulsive electrostatic potential and a short-range attractive potential to mimic vdW forces. All pairs of charged particles interact via a screened Debye–Hückel energy,

$$e_{\mathrm{el}}(r_{ij}) = \frac{z_i z_j e^2}{4\pi\varepsilon_\mathrm{r}\varepsilon_0}\exp(-\kappa r_{ij}) \ , \tag{1}$$

where r_{ij} represents the distance between monomer i and j, e is the elementary charge (1.6×10^{-19} C), ε_0 is the permittivity of a vacuum (8.854×10^{-12} C V m^{-1}), and z_i is the amount of charge on monomer i (+4). Free ions are not included explicitly in the simulation; nevertheless, their overall effect is described via the dependence of the inverse Debye screening length, κ^2, on the electrolyte concentration,

$$\kappa^2 = 1000\ e^2 N_\mathrm{A} \sum_i \frac{z_i^2 c_\mathrm{i}}{\varepsilon_0 \varepsilon_\mathrm{r} kT} \ . \tag{2}$$

Here N_A represents the Avogadro number (6.022×10^{23} mol^{-1}), c_i the ionic concentration, k the Boltzmann constant (1.3807×10^{-23} J mol^{-1} K^{-1}), and T the temperature (all the simulation runs were performed at 298 K). Because we consider chains at infinite dilution, the summation term covers the species of added electrolyte only and does not include particle charges or explicit counterion effects. vdW interactions are taken into account via a 12-6 Lennard-Jones potential,

$$e_{\mathrm{vdW}}(r_{ij}) = \varepsilon_{\mathrm{vdW}}\left[\left(\frac{r_0}{r_{ij}}\right)^{12} - 2\left(\frac{r_0}{r_{ij}}\right)^{6}\right] , \tag{3}$$

where $\varepsilon_{\mathrm{vdW}}$ is the minimum depth of the potential curve located at a distance r_0, which corresponds to the distance of two particles in contact. Positive values of $\varepsilon_{\mathrm{vdW}}$ mean that particle–particle contacts are energetically favorable. Because $\varepsilon_{\mathrm{vdW}}$ is a relative value, positive values of $\varepsilon_{\mathrm{vdW}}$ can result when attractive interactions between particle–particle contacts are stronger than those between particle–solvent contacts or when particle–monomer and/or solvent–solvent or monomer–solvent contacts are highly favored over particle–solvent or particle–monomer contacts.

The total energy which does not include the component originating from the entropy of the polymer chain for a given chain conformation is the sum of the electrostatic and vdW contributions,

$$\begin{aligned} E_{\mathrm{tot}} &= E_{\mathrm{el}} + E_{\mathrm{vdW}} \\ &= \frac{e^2}{0.41 \times 10^{-20}\varepsilon_{\mathrm{r}}\varepsilon_0}\sum_i \sum_{j>i} \frac{z_i z_j}{r_{ij}} \exp(-\kappa r_{ij}) \\ &\quad + \sum_{|i-j|>1} \varepsilon_{\mathrm{vdW}}\left[\left(\frac{r_0}{r_{ij}}\right)^{12} - 2\left(\frac{r_0}{r_{ij}}\right)^{6}\right] . \end{aligned} \tag{4}$$

The size of the polymer chain is characterized by

1. The reduced mean-square end-to-end distance,

$$\langle R_{\mathrm{ee}}^2 \rangle = \langle (r_N - r_1)^2 \rangle / \left(\sum_i^{N-1} l_{i,i+1} \right)^2 , \tag{5}$$

where $l_{\mathrm{i,i+1}}$ represents the bond length between the physical units i and $i+1$, and r_i is the position vector locating the ith segment of the chain (no distinction was made between particles and monomers).

2. The reduced mean-square radius of gyration,

$$\langle R_{\mathrm{g}}^2 \rangle = \frac{1}{N}\left\langle \sum_i^N (r_i - r_{\mathrm{cm}})^2 \right\rangle / (N-1)\ l_{\mathrm{m}}^2 , \tag{6}$$

with

$$r_{\mathrm{cm}} = \frac{1}{N}\sum_{i=1}^{N} r_i , \tag{7}$$

where l_{m} represents the mean bond length between the physical units of the chain, r_{cm} is the vector locating the center of mass of the chain, and $\langle\rangle$ denotes an ensemble average over a Monte Carlo run.

3. The Kuhn length, L_{k}, which is calculated using

$$\langle L_{\mathrm{k}} \rangle = \langle R_{\mathrm{ee}}^2 \rangle / \sum_i^{N-1} l_{i,i+1} , \tag{8}$$

where $L = \sum_{i=1}^{N-1} l_{i,i+j}$ represents the contour length of the chain.

MC simulations

We performed MC simulations according to the Metropolis algorithm [37] in the canonical ensemble. In this method successive "trial" chain configurations are generated to derive a reasonable sampling of low-energy conformations. After each elementary random movement, the Metropolis selection criterion is employed to either select or reject the move. If the change in energy, ΔE, resulting from the move is negative, the move is selected. If ΔE is positive the Boltzmann factor, p,

$$p = \exp\left[\frac{-\Delta E}{kT}\right] , \tag{9}$$

is computed and a random number, z, with $0 \leq z \leq 1$, is generated. If $z \leq p$, the move is selected. When $z > p$, the trial configuration is rejected and the previous configuration is retained and considered as a "new" state in calculating ensemble averages. That conformation is the one that is perturbed in the next step. The perturbation process is continued for a specified number of times (a typical run requires several million perturbations) until the conformation is energy-minimized and energy-equilibrated. To generate new conformations, the monomer positions are randomly modified by specific movements. They include three "internal" or elementary movements (end-bond, kink-jump, and crankshaft), and the pivot movement. The use of all these movements is very important to ensure the ergodicity of the calculations as well as the convergence on minimized conformations. A major difficulty is allowing the energy of the chain to be minimized gradually without trapping the chain structure in a local energy minimum. This problem is of particular importance when dense conformations have to be achieved owing to the fact that a few particle–particle contacts can lead to the formation of "irreversible" contacts that freeze the chain structures. To minimize the formation of structures in local minima and increase the chance of sampling new conformations, we used an approach which consists of using the most effective movements (internal or pivot) with regard to the chain conformation, at each step of the Monte Carlo procedure, to achieve a rapid and complete exploration of the configurational space of the chain. More computational details are given in Ref. [35], where the efficiency of this procedure is checked and verified with the formation of conformations such as pearl necklaces, cylinders, and dense coils. Nonetheless, in spite of the use of refined algorithms, such calculations required intensive computer processor speeds and memory capacities that have currently limited their applicability to single chains containing 100 physical units.

Results and discussion

Polymer chain conformations are investigated as a function of the ionic strength c_i and vdW potentials, ε_{vdW}. Five values of c_i are considered corresponding to 1-1 electrolyte concentrations of 1, 0.1, 0.01, 0.001, and 0M (unscreened limit). The values of ε_{vdW} are adjusted from 0 to $+25kT$ to cover a wide range of experimental and theoretically possible situations from extended to collapsed configurations depending on ionic strength. The overall effects of solution chemistry on the mean-square reduced radius of gyration, $\langle R_g^2 \rangle$, the end-to-end reduced length, $\langle R_{ee}^2 \rangle$, the Kuhn length, L_k, and the total energy, E_{tot}, of isolated chains are presented in Fig. 3 with the help of three-dimensional plots.

In the high-screened limit ($c_i = 0.1$, 1 M), by increasing ε_{vdW} up to $3kT$, $\langle R_g^2 \rangle$, $\langle R_{ee}^2 \rangle$, and L_k variations demonstrate that chains undergo a unique and sharp structural transition from swollen to dense conformations. The absence of long-range electrostatic repulsions causes dense conformations to be formed as a result of the attractive short-range interactions without any electrostatic force restraints. In the low-ionic-strength limit ($c_i = 0$, 0.001, 0.01 M), when ε_{vdW} interaction potentials are in the range 0–$10kT$, long-range electrostatic interactions between particles are predominant and force the chains to adopt extended configurations. Chain dimensions are characteristic of the stretched structures which are required to minimize the long-range repulsive interactions between particles since charges are separated by larger distances. By increasing further the intensity of the vdW interactions, competition between long-range repulsive and short-range attractive interactions becomes critical and results in the formation of compact structures whose conformations are strongly dependent on the initial chain configurations. As a result, two distinct chain transitions are experienced in this domain (Fig. 3 paths 1, 2). On the one hand, if extended structures are used at the beginning of the simulation runs, a smooth transition in polymer dimensions is obtained by increasing ε_{vdW} (Fig. 3a path 1). On the other hand, if swollen structures are used, over a small range of ε_{vdW} values chains experience large changes in their dimensions to the formation of extended conformations (Fig. 3a path 2). By considering the variations of the total energy, it is demonstrated that an extended-to-collapsed transition leads to the formation of "metastable" structures in local minima that have a lower energy than nearby conformations (extended) but a higher energy than more distant stable conformations (coils). As the final conformations are dependent on the initial ones ergodicity is thus not verified in such conditions. This aspect will be discussed further.

To gain insight into and to quantitatively characterize chain conformations, the ratio of the average square end-to-end distance and radius of gyration, $r = \frac{\langle R_{ee}^2 \rangle}{\langle R_g^2 \rangle}$, was calculated as a function of c_i and ε_{vdW} (Fig. 4). It is expected that in the rodlike limit $r = 12$, for self-avoiding-walk chains $r = 6.3$, for ideal or Gaussian chains $r = 6$, whereas for three-dimensional collapsed structures $r < 6$. According to Fig. 4, three regions could be defined. When vdW interactions are not predominant (region A), the plot of r versus c_i approaches the classical polyelectrolyte picture by following a linear dependence with r shown as a dotted line; however, in contrast to the predicted limit of $r = 12$ for rodlike chains when $c_i = 0$, we find a significant "bending" of the curve. The reason is that elementary movements used in the Monte Carlo sampling produce small orientational fluctuations along the chain backbone. As a result the rigid-rod limit is never completely reached at finite temperatures. This "entropic" contribution, which is expected to play a more and more pronounced role in increasing the chain length, wins on the Coulombic repulsions between particles and induces the formation of horseshoe conformations. Although the extrapolation of the solid line yields $r = 12$, the rodlike limit is expected to be practically inaccessible for flexible chains within our given sampling method.

In the limit of very strong vdW interactions, collapse transitions result in r values (region C) which are below the self-avoiding-walk or random-walk ones. As expected, these values reflect the formation of collapsed chains that are denser than the classical three-dimensional random walks.

In the limit of both strong electrostatic and vdW interactions evidence for the formation of exotic configurations in region B exists when extended conformations are used to start the calculations. To achieve a visual picture of chains, in particular, in region B, equilibrium conformations were extracted from our Monte Carlo calculation runs and represented as three-dimensional projections (Table 1) versus c_i and ε_{vdW}. Because of the lack of available space, extended polymers which have large dimensions have been reduced in size and appear smaller than they really are. The results in Table 1 demonstrate that neutral flexible chains with attached colloids have a large number of absolute conformations which are difficult to extract if one only considers macroscopic parameters such as $\langle R_{ee}^2 \rangle$, $\langle R_g^2 \rangle$, or L_k without a complete analysis of average eigenvalues. Clearly there is a range of parameters for which the polymer may exhibit a variety of anisotropic conformations: necklaces with compact beads joined by narrow strings, dumbbells, and cylinders. This large variety of conformations mainly results from the subtle balance of

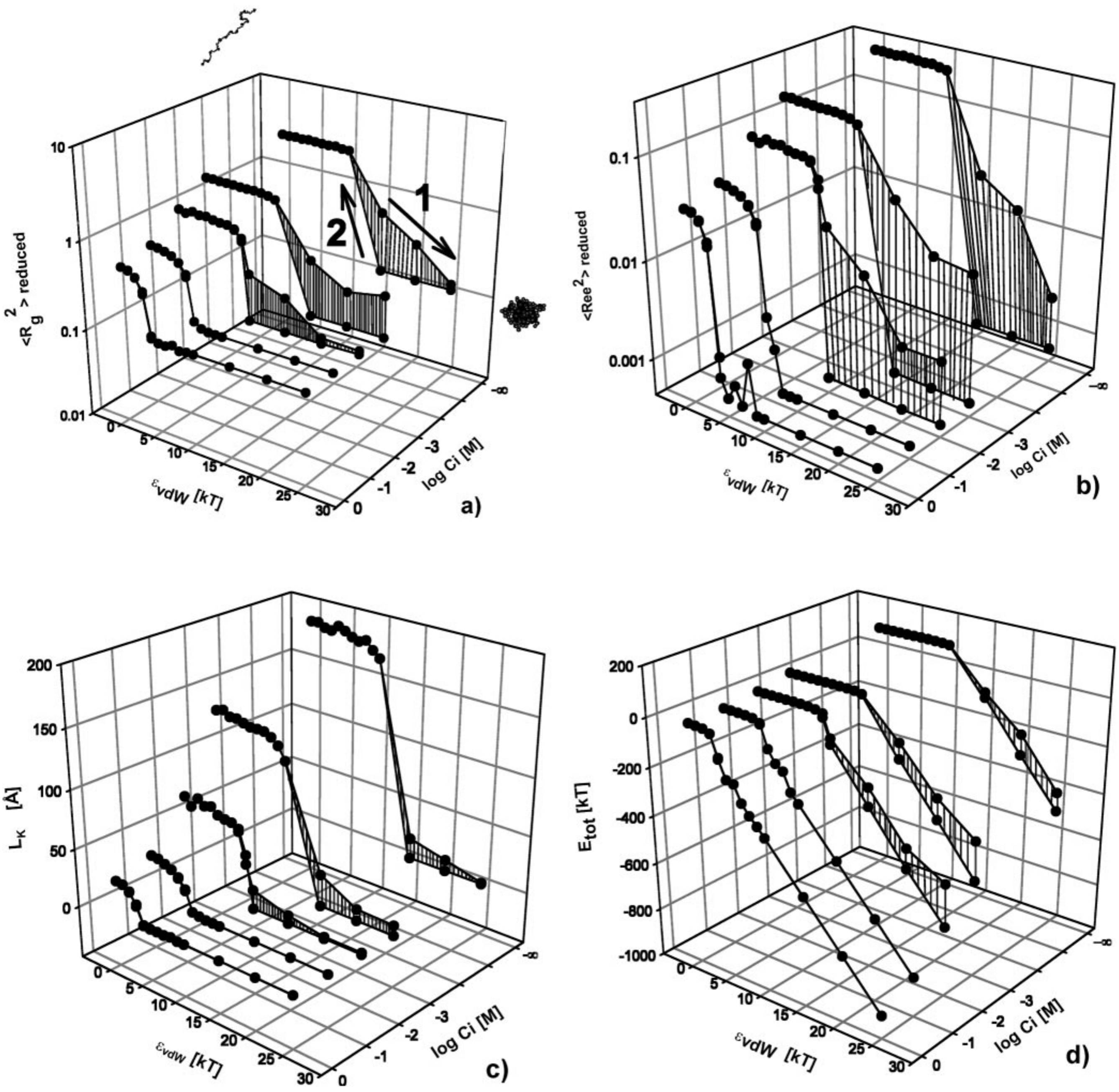

Fig. 3 $\langle R_g^2 \rangle$, $\langle R_{ee}^2 \rangle$, $\langle L_k \rangle$, and $\langle E_{tot} \rangle$ variations versus the vdW interaction and ionic concentration. By increasing the hydrophobic character of the chain and when the values are 1 or 0.1 M, sharp transitions from extended to coiled structures are observed. On decreasing the ionic strength two situations have to be considered depending on the initial conformations used in the calculations: sharp transitions to extended structures (*path 2*→) are observed using swollen configurations, whereas using extended chains, smooth transitions (*path 1*→) are achieved through the formation of metastable structures with regard to the corresponding $\langle E_{tot} \rangle$ values. The electrostatic interactions are expected to control the gradual transition to dense structures while passing by the formation of pearl necklaces in local minima

strong, short-range, attractive interactions and strong, long-range, electrostatic repulsions which forces the chain to adopt a global linear structure with dense parts or beads along it. Here one should note the similarity with the classical studies on the stability of charged droplets and/or hydrophobic polyelectrolytes: the long-range electrostatic interactions control the overall shape of the chains, causing them to maintain linear structures, whereas bead formation is controlled by the intensity of the short-range vdW interactions [38–41].

The transition between stretched chains and pearl-necklace conformations is gradually induced by increas-

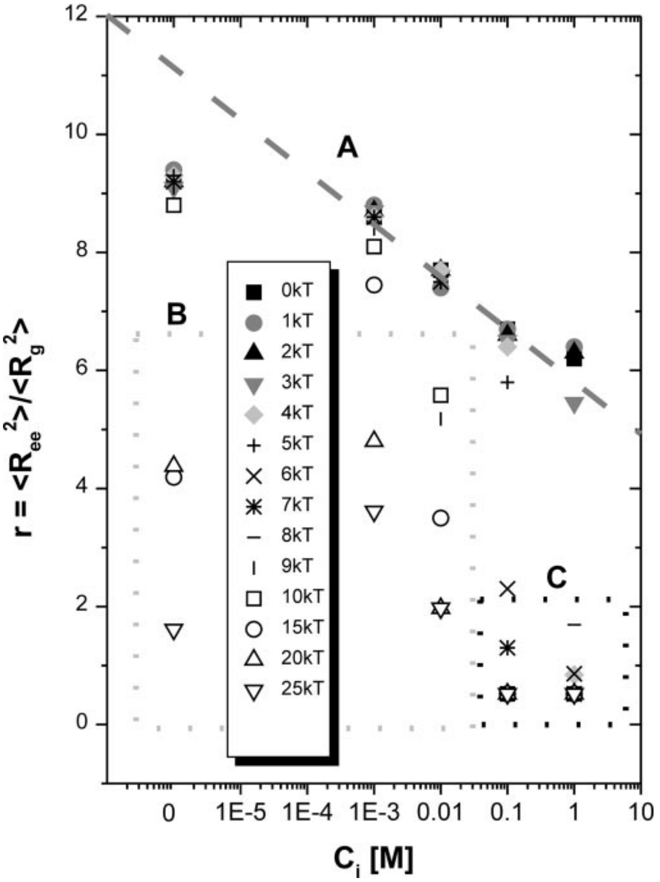

Fig. 4 The ratio of the end-to-end distance and the radius of gyration, $r = \langle R_{ee}^2 \rangle / \langle R_g^2 \rangle$, is plotted versus the ionic strength on a Logarithmic scale. $r = 12$ corresponds to a rigid rod, $r = 6$ corresponds to a random walk, whereas $r < 6$ corresponds to collapsed structures. When vdW interactions are weak i.e. $\varepsilon_{vdW} \leq 3kT$, r variations are close to the polyelectrolyte pictures by following a linear dependence with c_i (*region A*). The long-range nature of the Coulombic interactions stretches the chain. When vdW interactions are predominant collapsed structures are achieved in *region C* with $r < 6$. When the competition between the vdW and the electrostatic interactions becomes critical, r values are grouped in *region B* in contrast to the usual chain pictures (the extended polyelectrolyte with $r = 6 \rightarrow 12$, the rigid rod with $r = 12$, the coil with $r \ll 6$, and the self-avoiding walk with $r = 6$)

ing the intensity of the short-range vdW particle–particle interactions. The analysis of the dynamic trajectory during MC runs demonstrates that chains reduce their total energy by first splitting into dumbbell conformations, i.e. the formation of two end-to-end globules connected by a rigid string. Such a transition is due to the fact that the acceptance rate of elementary moves to form close particle–particle contacts is higher if moves are attempted at the chain extremities because of the decreasing electrostatic potential and the concomittant increase in the chain entropy with the distance to the center of the chains. However, one should bear in mind that the dumbbell and pearl-necklace structures which are formed in region B are representative of metastable structures only, i.e. in secondary minima, and that coils are more stable from an energetic point of view. Thus, one may wonder why ergodicity is not verified in region B, i.e. why two possible states are obtained depending on the initial chain conformation. This aspect is probably related to the difficulty in achieving transitions from the dumbbell (or pearl necklace) to the collapsed structures (Fig. 5a) with regard to the set of specific movements which are used in our calculations. In a situation where particles have been bound into dumbbells which are separated by a monomeric string, the MC sampling procedure efficiency or ability to join the dumbbells into a single coil is limited. Indeed owing to the finite distance between the two dumbbells, neither the pivot nor the internal movements are expected to gather all the particles in a simple manner. Large fluctuations in the chain dimensions and the energy are expected if the pivot algorithm is applied alone, whereas internal movements, which induce small local fluctuations in the chain dimensions, are not efficient enough to form new particle–particle contacts. Figure 5b, in which the convergence of the method is presented clearly, demonstrates that the so-called “metastable” conformations are not the result of fluctuations in the calculation process but are representative of equilibrated structures which are in a secondary minimum. At the present stage we cannot decide if these structures have an important physical meaning owing to the fact that our MC sampling method is not suitable for overcoming the energetic barrier to pass from the pearl-necklace conformation to more stable collapse conformations. The question is then to know whether the same behavior could be obtained using experiments or computer simulations such as molecular or Brownian dynamics, for example.

In the limit of highly screened electrostatic interactions (c_i = 0.1, 1M) and ε_{vdW} interactions in the range 4–25kT (region C) dense spherical coils are formed. With regard to the configurations presented in Table 1, we can obviously note a specific spatial ordering of both monomers and particles, i.e. particles clearly grouped together and surrounded by a shell mainly composed of monomers. To gain quantitative insight into the chain structures, i.e. the radial distribution of monomers and particles, the pair distribution functions [monomer–monomer, P_{mm}(r), and particle–particle, P_{pp}(r)] were calculated. The peak pair distribution functions for extended, swollen, and collapsed structures are shown in Fig. 6. As expected, the width and peak positions decrease with increasing vdW interactions or with increasing ionic strength (Fig. 6a). The large and narrow peaks when c_i = 1M and ε_{vdW} = 2kT (Fig. 6c) mean that both the particle and the monomer densities are higher in such conditions. By comparing the two peak positions of the collapsed structure it is demonstrated that the polymeric shell is obviously surrounding a core

Table 1 Chain conformations versus ionic concentration and attractive particle–particle interaction potentials. *Domain A*: a self-avoiding walk and an extended conformation are formed because of the predominant role of the electrostatic repulsions between particles. *Domain B* (*shaded cells*): using an extended configuration at the initial step of the Monte Carlo calculations, metastable structures are formed (pearl necklaces, dumbbells). These structures are trapped into conformations that have a lower energy than extended structures but a higher energy than the collapsed ones, i.e. they are in secondary minima. *Domain C*: van der Waals interactions are now predominant. Chains adopt collapsed conformations. Because of the lack of available space, extended chains which are large dimensions have been reduced in size and subsequently appear smaller than they really are

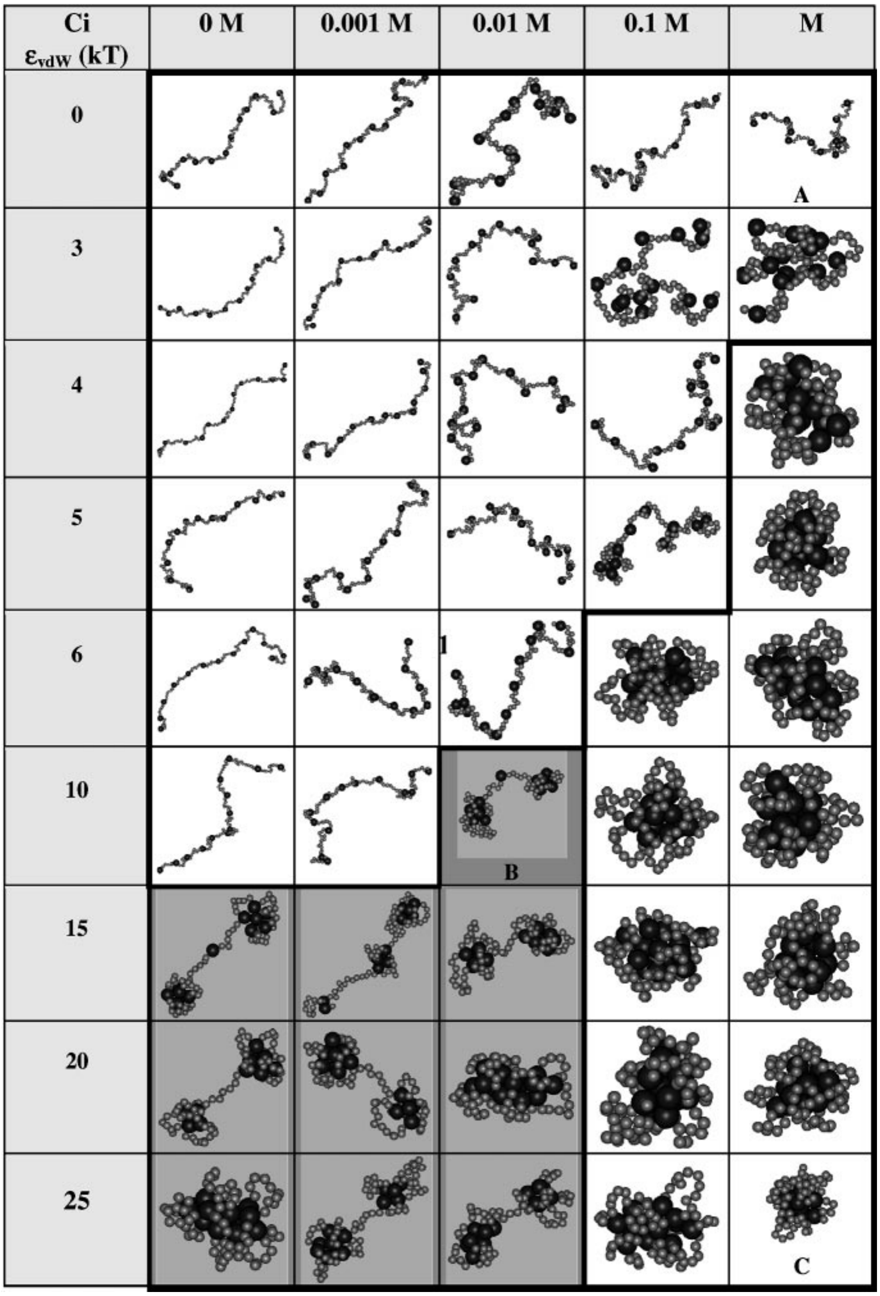

made of particles. As a result, collapsed structures and partially stabilized with the polymer, the polymeric loops protruding in the "liquid" phase providing steric stabilization.

Outlook and conclusion

Using a Debye–Hückel and a Lennard-Jones potential approach to describe the destabilization of a large neutral and flexible chain on which small particles are attached, a possible cascade transition from extended conformations to dense coils while passing by the formation of metastable dumbbell structures is demonstrated. Transitions from extended configurations to coils, which are continuous in all cases with increasing particle–particle interactions, become more prominent with increasing charge-screening. With regard to the possible formation of dumbbells, MC simulations demonstrate the dual nature of this process. On the one hand, the short-range attractive nature of the vdW forces tends to coil the chains, whereas, on the other

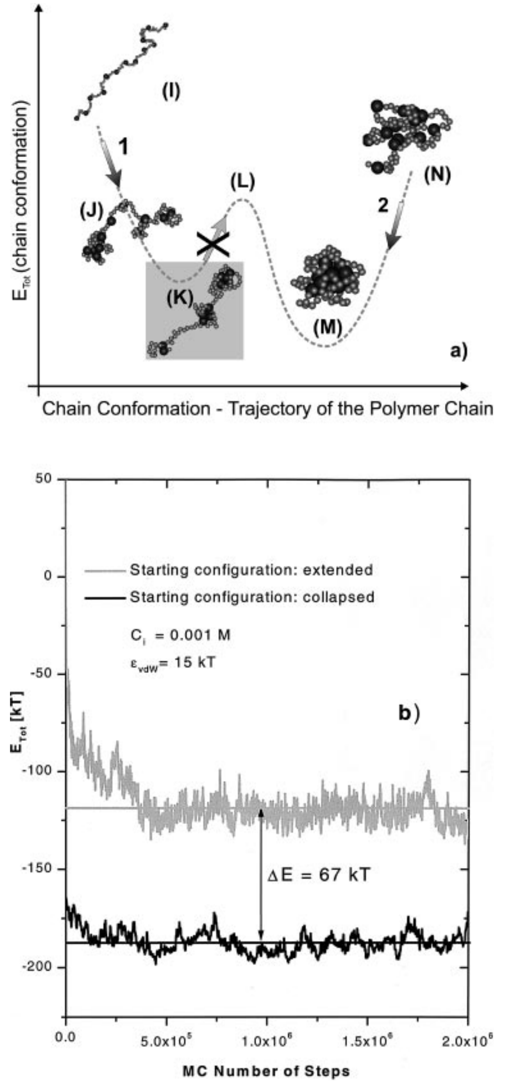

Fig. 5 a Schematic representation of the total energy trajectory of the particle–chain system when the solution chemistry is adjusted to produce both strong electrostatic repulsions and vdW attractions (Table 1, region B). Starting the calculations with extended conformations results in a local minimum, *K* (region B), which is not the global minimum, *M*. The Monte Carlo search algorithm (minimization procedure), which uses a set of elementary movements, is not specifically designed to push the system over barriers but down into the nearest valley of conformation *I*. Modified strategies are thus needed to search conformational space more throughly and to climb and cross conformational energy barriers such as *L* to go into the primary minimum *M*. Using swollen conformations, *N*, the MC search algorithm converges directly to the primary minimum, *M* without passing by the formation of dumbbell structures. **b** Dependence between the energy E_{tot} and the MC iteration number. It is demonstrated that the so-called "metastable" conformations, *K* (*gray line*), are not the result of fluctuations in the calculation process but are representative of equilibrated structures which are in a secondary minimum. The *black line* represents structures of type *M* which are in a primary minima

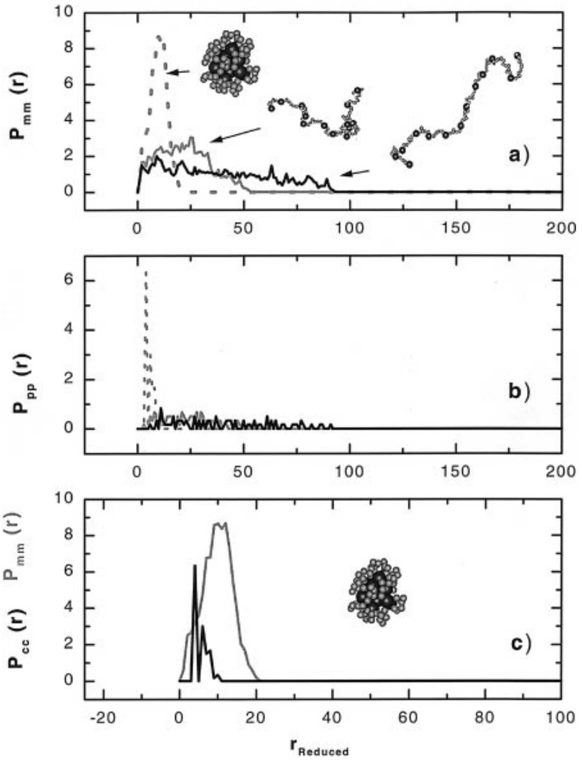

Fig. 6a–c Pair correlation functions versus the reduced distance. **a** The monomer–monomer pair correlation function for a collapsed (*dotted gray line*), a swollen (*gray line*), and a stretched conformation (*black line*). The mean distance decreases with increasing vdW interactions. **b** The particle–particle pair distribution function. **c** The pair correlation functions of a collapsed structure. By comparing the two peak positions it is clearly demonstrated that the particles are embedded in a polymeric shell

hand, long-range Coulombic repulsive forces cause the chains to elongate.

Although our MC procedure was carefully extended to increase the success rate of the elementary movements to sample all the chain conformational space, i.e. the formation of both dense and stretched domains within a single chain, the present investigation demonstrates that owing to the number of steps required to achieve pearl-necklace structures (several million) MC suffers from today's limited simulation time as well as from sampling efficiency with regard to nonergodicity problems. Modified strategies are still needed to search the conformational space more throughly and to climb and cross conformational energy barriers. In addition, a more realistic and quantitative description of the interaction potentials between our physical units could require a more sophisticated model involving explicit counterions as well as solvent molecules to correctly treat solute–solvent–salt interactions so that local electrostatic effects, such as counterion condensation, could have their full effect.

One of the salient results of this work concerns the possible effects of such collapse transitions on the kinetics of flocculation and floc structures involving large flexible chains and comparatively small colloidal particles. It is expected that the extent of flocculation will depend, prior to the formation of large flocs composed of several chains, on the chain reconformation process in the first flocculation regime, i.e. during the formation of aggregates composed of single chains with several particles adsorbed on them. In particular, if particle–particle attraction is strong, coils composed of particles surrounded by a polymer layer could be formed. This collapse transition could profoundly decrease the aggregate formation kinetics by steric hindrance, subsequently preventing the particles from acting as ligands between the chains in a second flocculation regime.

Although the extent of flocculation depends on the solution chemistry (ionic strength, temperature, pH) and on the particle and the chain chemistry (surface charge density, Hamaker constant), the essential question is whether chain reorganization before or during the formation of large aggregates occurs sufficiently fast to strongly modify the flocculation processes. It is worth noting that chain reorganization could also depend on the total number of adsorbed particles and hence on the distances between the hydrophobic parts of the chain, on the chain/particle relative size, and obviously on the chain intrinsic flexibility.

Hence, our theoretical description of the different steps of flocculation processes is still part of a great challenge and polymer-chain–particle interaction modeling still leaves much room for progress in order to completely understand these reconformation processes and their effects and to develop a general theory of flocculation processes consistent with experimental modeling, which is still needed to bridge the gap between simulations and environmental systems, such as flocculation in natural waters or wastewater treatment.

A future report will consider both hydrophobic interactions and electrostatic interactions between monomers and particles, as well as internal constraints to mimic chain flexibility. The particles will be permitted to move along the chains by considering a reversible adsorption process. This effect could be important in the collapsed state where the particles strongly attract each other. For the present, we have concentrated on the qualitative and quantitative effects of interacting particles associated with connectivity and flexibility on a simple self-avoiding-walk neutral chain leaving us with two single adjustable parameters.

Acknowledgements We wish to thank N. Parthasarathy and J. Buffle for helpful discussions. This work was supported by the Fonds National Suisse (projects 2000-043568.95/1). The calculations reported here were performed at the Computer Center of the University of Geneva, which is acknowledged for providing computation time.

References

1. Napper DH (1983) Polymeric stabilization of colloidal dispersions. Academic, New York
2. Stumm W (1987) Aquatic surface chemistry. Wiley, New York
3. Buffle J, Van Leeuwen HP (1993) Environmental particles. IUPAC Series on Environmental Analytical and Physical Chemistry. Lewis, New York
4. Wilkinson K, Stoll S, Buffle J (1995) Fresenius Z Anal Chem 351:54
5. Wilkinson K, Balnois E, Leppard GG, Buffle J (1999) Colloids Surf A 155:287
6. Buffle J, Wilkinson K, Stoll S, Filella M, Zhang J (1998) Environ Sci Technol 32:2887
7. Fillela M, Buffle J (1993) Colloids Surf A 73:255
8. Perret D, Newman M, Negre JC (1994) Water Res 28:107
9. Elaissari A, Pefferkorn E (1990) J Colloid Interface Sci 141:522
10. Ouali L, Pefferkorn E (1994) J Colloid Interface Sci 168:315
11. Stoll S, Buffle J (1996) J Colloid Interface Sci 180:548
12. Vicsek T, Family F (1984) Phys Rev Lett 52:1669
13. Meakin P, Vicsek T, Family F (1985) Phys Rev B 31:564
14. Lindsay H, Lin M (1987) Faraday Discuss Chem Soc 83:153
15. Mandelbrot B (1983) The fractal geometry of nature. Freeman, New York
16. Jullien R, Botet R, Mors PM (1987) Faraday Discuss Chem Soc 83:125
17. Family F, Landau DP (1984) Kinetics of aggregation and gelation. North-Holland, Amsterdam
18. Jullien R, Botet R (1987) Agregation and fractal Aggregates. World Scientific, Singapore
19. Meakin P (1998) Fractals, scaling and growth far from equilibrium. Cambridge University Press, London
20. Pincus PA, Sandroff CJ, Witten TA (1983) J Phys 45:725
21. Alexander S (1977) J Phys 38:977
22. Granfeldt MK, Jönsson B, Woodward CE (1991) J Phys Chem 95:4819
23. Currie EPK, van der Gucht J (1988) Langmuir 14:5740
24. Cabane B, Duplessix R (1985) Colloids Surf 13:19
25. Cabane B, Wong K, Wang TK, Lafuma F, Duplessix R (1988) Colloid Polym Sci 266:101
26. Wong K, Cabane B, Duplessix R (1988) J Colloid Interface Sci 123:466
27. Wong K, Cabane B, Somasundara P (1988) Colloids Surf 30:355
28. Currie EPK, van der Gucht J (1988) Langmuir 14:5740
29. Dickinson E, Euston S (1991) J Chem Soc Faraday Trans 287:2193
30. Dickinson E (1990) The structure, dynamics and equilibrium properties of colloidal systems. Kluwer, Amsterdam
31. Nowicki W, Nowicka G (1997) Can J Chem 75:1248
32. Nowicki W, Nowicka G (1995) Colloid Polym Sci 273:298
33. Molski A, Nowicki W (1989) Colloid Polym Sci 267:506
34. Stoll S, Buffle J (1998) J Colloid Interface Sci 205:290

35. Chodanowski P, Stoll S (1999) J Chem Phys 111:6069
36. Vermeer R (1996) Thesis. Wageningen, Netherlands
37. Metropolis N, Rosenbluth AW (1953) J Chem Phys 21:1087
38. Rayleigh L (1882) Philos Mag 14:184
39. Dobrynin AV, Rubistein M, Obukhov S (1996) Macromolecules 29:2974
40. Noguchi H, Yoshikawa K (1998) J Chem Phys 109:5070
41. Yoshikawa K, Yoshikawa Y, Yoshiyuki K, Kanbe T (1997) J Am Chem Soc 119:6473